Long-term Variability in the Seasonality of Eastern Boundary Current (EBC) Systems: an Example of Increased Upwelling from the California Current

Franklin B. Schwing

Roy Mendelssohn

Pacific Fisheries Environmental Group
(PFEG)
1352 Lighthouse Avenue
Pacific Grove
CA 93950-2097
USA

Abstract

State-space statistical models are applied to long environmental time series of monthly northward wind stress, sea surface temperature (SST), coastal salinity (SSS) and coastal sea level (SL) from the west coast of North America. We describe the models, which use a combination of Kalman filtering and maximum likelihood methods to estimate a non-parametric non-linear trend, a non-stationary and statistically non-deterministic seasonal signal, and an autoregressive term. The models effectively separate the seasonal signals from the long-term trends.

The seasonal series are examined for behavior consistent with increasing coastal upwelling during April--July, the 'upwelling season'. We test the A. Bakun's hypothesis that equatorward wind stress, hence upwelling, has been increasing in eastern boundary current systems over the past several decades, presumably in response to a pattern of long-term global warming. Over a region of the California Current System (CCS) where coastal upwelling is a dominant process (32-40°N), wind stress,

SST, salinity and sea level all show strong evidence of a systematic intensification of upwelling during April-July. Equatorward stress and salinity display a strong linearly increasing tendency over time, while SST and sea level decrease significantly. The four parameters are significantly correlated in a manner consistent with increased upwelling as well; SST and sea level have decreased, and salinity has increased, coincident with strengthening equatorward stress.

To check that these results are unique to the seasonal model components, time series of April-July averages from the monthly observations and model trend series were examined. The trends in the region 32-40°N suggest a linear tendency for increasing equatorward stress (in agreement with the seasonal tendency), but warmer SST (opposite the seasonal and the expectation of greater upwelling), and closely match the tendencies in the observations. The linear tendencies of the SST and stress trends are generally an order of magnitude greater than in the seasonal tendencies. Thus the long-term trend in SST masks the cooling effect of increased seasonal upwelling, and the trend in equatorward stress suggests an artificially large seasonal increase in the observed spring and summer stress. A key to identifying these patterns has been the ability to separate the long-term non-linear trend, using the state-space models, which mask the signal of increased upwelling in the observations.

RÉSUMÉ

Des modèles Espace-Etat sont appliqués à des séries environnementales de la côte ouest de l'Amérique du Nord : tension méridienne du vent, température de surface (SST), salinité côtière (SSS) et niveau de la mer (SL). Ces modèles estiment de façon non paramétrique une tendance non linéaire, un signal saisonnier non stationnaire et statistiquement non déterministe et un terme autorégressif par la méthode du filtre de Kalman et du maximum de vraisemblance. Il est ainsi possible séparer les signaux saisonniers des tendances de long terme.

D'après A. Bakun, la tension méridienne du vent dans les écosystèmes d'upwelling aurait augmenté durant les dernières décennies probablement à cause de la tendance au réchauffement global. Le comportement de diverses séries saisonnières pendant la saison d'upwelling a été examiné dans la région de l'écosystème du courant de Californie où l'upwelling côtier est un processus dominant (32-40 °N). L'évolution de la tension du vent, de

la température de surface, de la salinité et du niveau de la mer montre que durant la saison d'upwelling d'avril à juillet, il y a une intensification systématique de l'upwelling. La tension méridienne du vent et la salinité présentent une forte augmentation dans le temps tandis que la température de surface et le niveau de la mer diminuent significativement. Le sens de ces évolutions correspond bien à une intensification de l'upwelling.

Pour vérifier que ces résultats sont bien spécifiques de la composante saisonnière du modèle, la composante tendancielle et la moyenne des observations mensuelles sur la période avril-juillet ont également été examinées. Pour ce qui concerne la tension méridienne du vent, la tendance à long terme, tout comme la tendance saisonnière, vont dans le sens d'une augmentation. Par contre, la composante tendancielle et les observations sur la période avril-juillet de la température de surface montrent l'existence d'un réchauffement à long terme alors que c'est un refroidissement qui est constaté dans la composante saisonnière des températures de surface. Que ce soit pour la tension méridienne du vent ou pour la température de surface, l'ordre de magnitude des variations est plus grand pour la tendance à long terme que pour la tendance saisonnière. Ainsi, la tendance au réchauffement à long terme de la température de surface masque l'existence d'un refroidissement accru durant la saison d'upwelling. De même, la tendance à l'augmentation à long terme de la tension méridienne du vent suggère que la croissance observée durant la saison d'upwelling soit en partie artificielle. Elle relève pour partie d'un phénomène plus général et non pas d'un phénomène saisonnier. Les modèles Espace-Etat qui permettent d'extraire préalablement des données observées les tendances à long terme sont un instrument clé pour pouvoir identifier correctement l'évolution des phénomènes saisonniers.

INTRODUCTION

Climate variability on very large time (century) and space (global) scales impacts – or has the potential to impact – marine ecosystems at a variety of smaller scales. A number of recent papers have explored the patterns and dynamics of fluctuations embedded within the long-term, globally-integrated tendency commonly referred to as climate change ((Trenberth, 1990; Mann and Park, 1993, 1994; Graham, 1994; Miller *et al.*, 1994; Roemmich, 1992; Trenberth and Hurrell, 1994; Ware, 1995) to name but a few). However these studies have concentrated on large-scale temporal oscillations, generally on decadal scales; fewer examples (cf. Parrish *et al.*, 1981) describe variability on sub-basin (i.e., 100-1000 km) space scales.

In a particularly striking example of how global climate change may be affecting ocean conditions on smaller scales, Bakun (1990) postulates that under the scenario of global warming, continental air masses will warm more rapidly than oceanic air masses, leading to an intensified summer continental atmospheric low, a greater cross-margin pressure gradient between the continental low and higher pressure over the cooler ocean, stronger equatorward wind stress and increased coastal upwelling along eastern ocean boundaries. The effect on eastern boundary current (EBC) systems could be significant, because of the highly productive nature of these ecosystems and their potentially important role in the global CO_2 budget.

Upwelling is not a temporally continuous or spatially uniform process, but displays periods of favorable conditions for upwelling and downwelling (as well as substantial interannual variability), and has a distribution that suggests certain geographical sites as being more conducive to upwelling (Rosenfeld *et al.*, 1994). Empirical studies of upwelling and its effects on biological production suggest that optimal fisheries production occurs within a limited range of wind speeds; at speeds greater than about 5-7 m/s the biomass of small pelagic fish decreases (Cury and Roy, 1989). This has resulted in an ecosystem that is tuned to these variations. Any long-term changes in the seasonal patterns of upwelling, their intensity or the duration of upwelling events could have dramatic implications to EBC ecosystems and their living marine resources.

In this and in a companion paper (Schwing *et al.*, this vol.), we take advantage of a unique data set of long (multi-decadal) coastal environmental time series from along the west coast of North America, to evaluate changes in both the long-term trend and in the seasonal variability of EBC atmospheric forcing and the oceanic response. We were able to perform this evaluation by applying state-space models (Shumway, 1988, Chapter 3; Harvey, 1989; and Durand and Mendelssohn, this vol.) to separate the seasonal component from the long-term trend in a variety of California Current System (CCS) environmental time series.

Here we examine the variability in the seasonal component on climate (decadal and longer) scales, and in particular we test the hypothesis of Bakun (1990) that equatorward wind stress in spring and summer, hence upwelling, has been increasing in EBCs over the past several decades, presumably in response to a long-term global warming trend.

1. METHODS

1.1. Time series

The monthly-averaged time series described here were generated from a variety of sources. The primary data base was the Comprehensive Ocean-Atmosphere Data Set (COADS). The COADS contains almost 100 million reports of ocean surface conditions, mostly taken by ships-of-opportunity. The data have been collected, quality-controlled and put into common formats and units (Slutz *et al.*, 1985; Woodruff *et al.*, 1987). Data were extracted using the CD-Rom-based version of COADS and the CODE extraction program described in Mendelssohn and Roy (1996). The CD-Rom version contains Release 1 of COADS for the period 1854-1979 and the Interim release for 1980-1990, in CMR5 format. The wind data are marked as estimated, for winds approximated using the Beaufort scale; as measured, for anemometer or buoy measurements; or as unknown, when the measurement method and device were not known. Only wind data marked as

estimated or unknown were used in forming the mean series, to avoid as much as possible the known bias in the data due to an increase over time in the use of anemometers to measure the wind (Cardone *et al.*, 1990; Isemer, 1992; Wu and Newell, 1992). Based on statistics from the data set, each observation for each parameter has been flagged as to the 'quality' of the observation (Slutz *et al.*, 1985). Poleward (northward) pseudo-stress, henceforth referred to as wind stress, was derived by squaring the northward wind component from each record extracted prior to monthly averaging. Spatial regions approximately two degree latitude by four degree longitude were defined based on a combination of ecological and oceanographic features as well as data density, and time series of poleward wind stress and sea surface temperature (SST) were calculated for each region (Fig. 1, Table 1) from the monthly means of each variable. To exclude possibly erroneous observations, all COADS data outside of their 'wide interval' (roughly equal to three standard deviations) were excluded from the averaging. These geographic boxes are referred to in terms of their central latitude (e.g., 23°N refers to the 22-24°N COADS box). The time period of extraction is 1946-90.

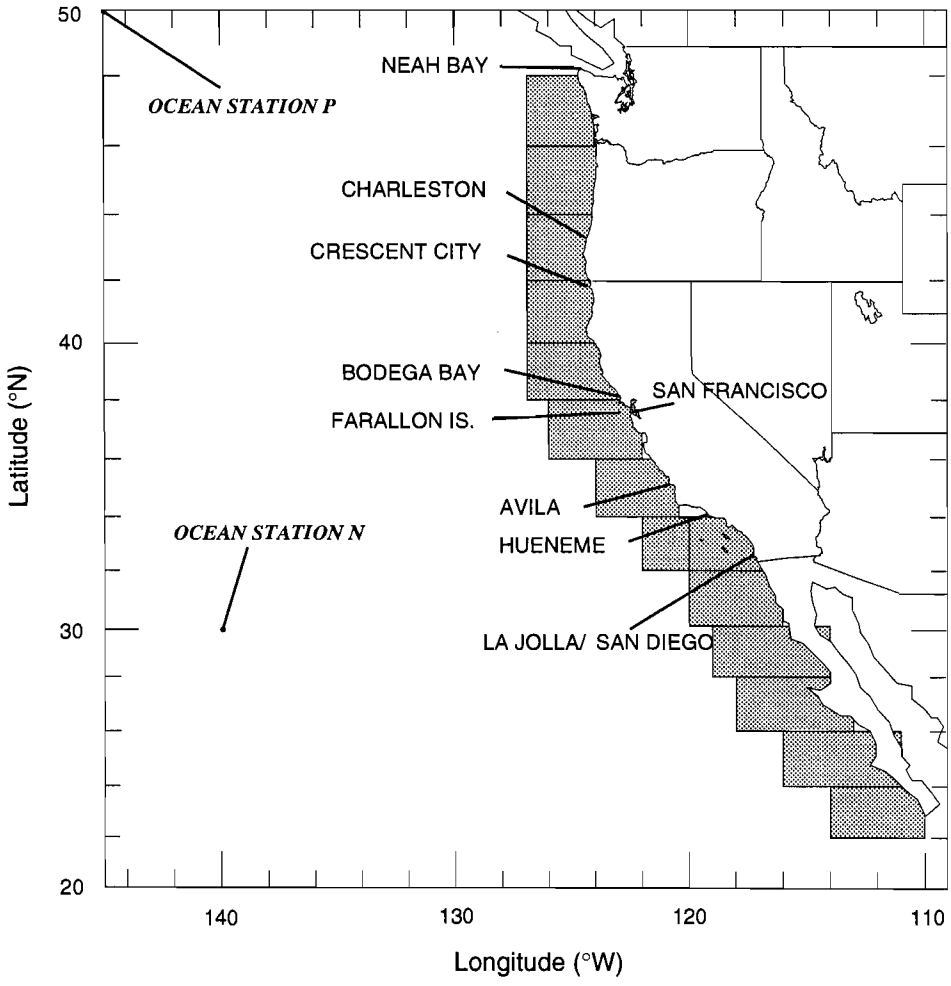

Fig. 1: Locations of COADS 2° boxes (shaded), and coastal stations from which monthly time series were generated. Locations of Ocean Stations P and N also are shown.

COADS LAT. (°N)	COADS LONG. (°W)	SHORE & OCEAN STATIONS (°N)	SST	SSS	SL
46-48	124 - 127	Neah Bay (48°22')	1935-92	1936-92	1934-92
44-46	123.5- 127	—	—	—	—
42-44	124 - 127	Charleston (43°21')	1966-92	—	—
40-42	123 - 127	Crescent City (41°45')	1933-92	1934-92	1933-92
38-40	122 - 127	Bodega Bay (38°19')	1957-92	1975-92	—
36-38	122 - 126	Farallon (37°25')	1925-92	1925-92	1915-92
34-36	120.5- 124	Avila (35°10')	1945-92	1945-79	—
S.C. Bight	116 - 120	Hueneme (34°09')	1919-87	1919-63	—
		La Jolla (32°52')	1916-92	1926-92	1915-92
30-32	116 - 120	—	—	—	—
28-30	114 - 119	—	—	—	—
26-28	113 - 118	—	—	—	—
24-26	111 - 116	—	—	—	—
22-24	110 - 114	—	—	—	—
—	—	Station P (50°N,145°W)	1950-92	1956-92	—
—	—	Station N (30°N,140°W)	1954-74	—	—

Table 1: Dimensions of COADS boxes containing derived monthly averaged equatorward wind stress and SST (for period 1946-1990), and selected shore stations within the COADS boxes. Years for monthly averaged time series of coastal SST, coastal salinity (SSS) and sea level (SL) shown.

Shore-based monthly SST and salinity (SSS) time series were averaged from daily observations made by volunteers, which were sent to the Marine Life Research Group, Scripps Institution of Oceanography (Walker *et al.*, 1993). SSTs were reported to the nearest 0.1°C at most sites. The observations are accurate to about ±0.2°C. Salinities were determined at Scripps from daily sea water samples using an inductive salinometer. Daily observations were quality controlled prior to the monthly-averaging. The number of daily values varied from 15-20/month (and as little as 10/month during winter months) at some of the northern stations (e.g., Farallon, Crescent City), to nearly complete coverage (e.g., La Jolla). Since 1979, NOAA/NOS has measured density with a hydrometer at Neah Bay and Crescent City. Salinities were back-calculated from these monthly-averaged densities. The locations of shore stations are shown in Fig. 1 and Table 1.

Monthly-averaged time series of sea level (SL) were supplied by NOAA/NOS, some through the Pacific Climate (PACLIM) data base (Cayan *et al.*, 1988). Long SL series are available at four sites (Fig. 1, Table 1). With a few exceptions, missing values in the shore time series were sparse and of only one to a few months duration. The time- and space-averaging for the COADS series were selected to ensure no missing observations while maximizing resolution. Months with no data were included in the analysis; the model fits through periods of missing data.

1.2. State-space statistical model

To estimate a time-varying (i.e., nonstationary) seasonal component for each observed time series, we assume that each observation y(t) is the sum of four components

$$y(t) = T(t) + S(t) + I(t) + e(t),\ t=1,T \quad (1)$$

where, at time *t*, *T(t)* is the unobserved time-dependent mean-level (trend), *S(t)* is the seasonal component, *I(t)* is the irregular term (stationary but autocorrelated), and *e(t)* is the stationary, uncorrelated component which here can be viewed as "observation" or "measurement" error.

As given, the model in Equation (1) is not uniquely specified, so meaningful solutions are not possible. To obtain a meaningful solution some constraints must be placed on the 'smoothness' of each component in the decomposition. Several methods for constraining the components have been suggested in the literature, related to 'smoothing spline' estimation of unknown functions. (The methodology is discussed in some detail in Durand and Mendelssohn, this vol.). For our analysis, we constrain the first differences of the trend component (the discrete equivalent of the first derivative) to be normal random variables with a mean of zero and unknown variance, that is:

$$\nabla^k T(t) \sim N(0, \sigma^2_T) \quad (2)$$

The seasonal component is defined by constraining the running sum of the seasonal component to be a normal random variable with a mean of zero and unknown variance, that is (assuming *s* periods in a season; e.g., *s=12* for monthly data, *s=4* for quarterly data)

$$\sum_{i=0}^{s-1} S(t-i) \sim N(0, \sigma^2_S) \quad (3)$$

The irregular term *I(t)* is assumed to be a p-th order autoregression, that is

$$I(t) \sim \sum_{i=1}^{p} \phi_i I(t-i) + \varepsilon(t) \quad (4)$$

$$\varepsilon(\tau) \sim N(0, \sigma^2_I) \quad (5)$$

and the observation errors are assumed to be zero mean, independent, identically distributed as

$$e(t) \sim N(0, \sigma^2_e),\ t=1,T. \quad (6)$$

In our analysis, a first order autoregressive model is used throughout for the irregular term. The entire model can be written in state-space format and solved using a combination of Kalman filtering and maximum likelihood (see Durand and Mendelssohn, this vol., for details).

The flexibility of this parameterization can be understood best by examining the limits of the trend and seasonal components at the extreme values of their variances (zero and infinity) when the other components have been removed (the partial residual series). If the seasonal and irregular terms were somehow known, then the algorithm would estimate a smoothed version of the observed series minus the seasonal and irregular components. When the trend variance (σ^2_T) is zero, this smoother is simply a linear least-squares fit to the partial residual series. When the trend variance approaches infinity, then the smoother simply interpolates the partial residual series.

If the trend and irregular were removed from the data, then the algorithm calculates for the seasonal component given by

Equation (3), a smoothed version of the *s*-period running sums of the partial residual series, where the amount of smoothing applied is the same throughout the series. (This implicitly will smooth the s-period differences also.) When the seasonal variance (σ^2_s) is zero, the result is the monthly means of the partial residual series. When the seasonal variance approaches infinity, then the result again interpolates the partial residual series.

Likewise, if the trend and seasonal components were known, then the irregular term estimates a *p*-th order autoregressive model to the partial residual series after the trend and the seasonal were removed. While the algorithm used in this paper estimates the components simultaneously, this 'backfitting' type approach of recursively smoothing the partial residual series could be used with other smoothing algorithms. Examples of the partial residual series and the estimated components for several series are given in Durand and Mendelssohn (this vol.).

The means of the monthly seasonal model time series for April-July (the upwelling 'season') were calculated in each year to produce the time series analyzed and described below (i.e., each annual value represents the average of the April-July period in that year). These series will henceforth be referred to as the upwelling time series.

2. RESULTS

2.1. Upwelling time series

The mean wind stress and SST for April-July (the upwelling 'season') were calculated in each year from the seasonal model series for the COADS 2° boxes. Plots of these upwelling time series are shown in Fig. 2. In most boxes, there is a close positive correlation between stress and SST. This is reflected in the linear correlations between these variables (Fig. 3, Table 2). There also is considerable consistency in stress and SST between adjacent boxes.

Seasonal series over most of the CCS region south of about 40°N display a fairly linear tendency of increasing equatorward (more negative) stress and decreasing SST over time. Both tendencies reverse north of 40°N, although stress again becomes more equatorward over time north of 44°N. The strong positive correlation between stress and SST also decreases in this northern region (Fig. 2, Table 2), and is actually significantly negative ($p<0.01$) over 44-48°N. South of 30°N the pattern of decreasing stress and SST changes gradually from a 'bowl-shaped' series to a linear increasing trend, similar to that noted north of 40°N.

In summary, upwelling wind stress has become more strongly equatorward over time in the region 32-40°N and north of 44°N. SST has become significantly cooler during the upwelling season between 30 and 40°N. The linear correlation between stress and SST is statistically significant and positive south of 40°N. Over the region 32-40°N, from about the U.S.-Mexico border to Cape Mendocino (shaded region in Fig. 3), the linear relationship between stress, SST and time are all consistent with increased upwelling.

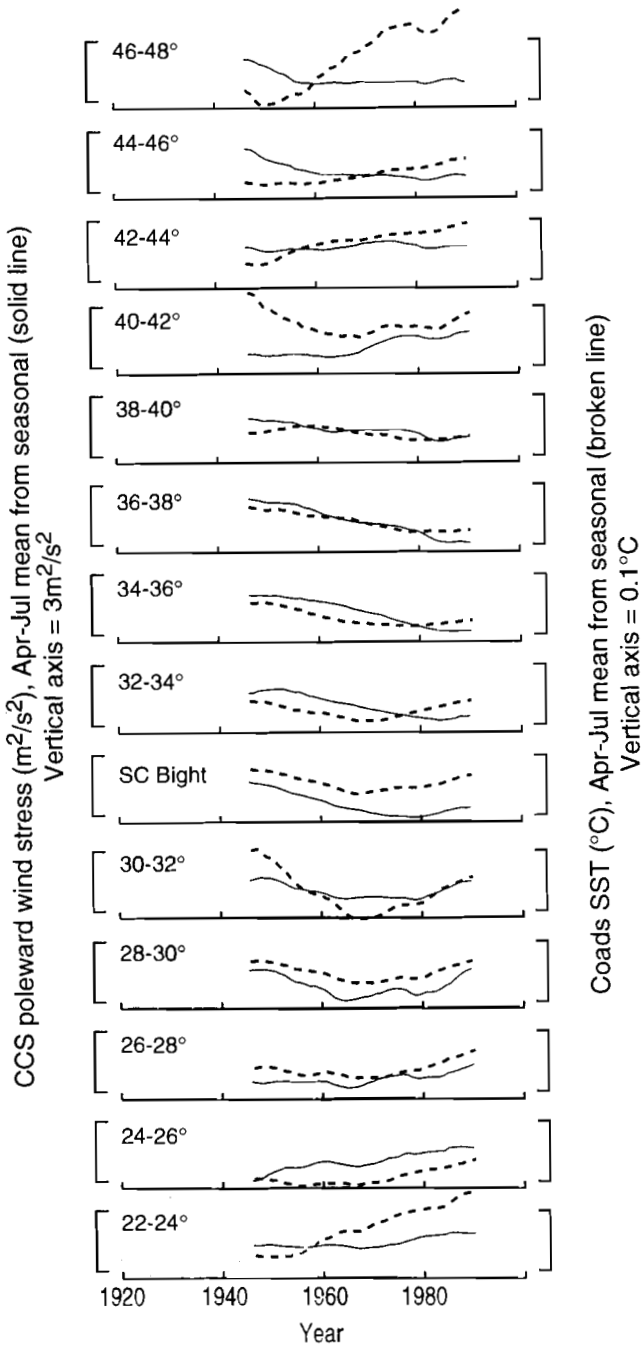

Fig. 2: Time series plots of 'upwelling' series (April-July averages from seasonal model components) for poleward wind stress (solid lines) and SST (dashed lines), for COADS 2° boxes. Vertical axes denote $3m^2/s^2$ and 0.1°, respectively.

LATITUDE	τ vs. YEAR (Apr-Jun)			SST vs. YEAR (Apr-Jun)			SST vs. τ (Apr-Jun)			SST vs. τ (Oct-Jan)		
	r	b(10^{-2})	±99%CI	r	b(10^{-3})	±99%CI	r	b(10^{-2})	±99%CI	r	b(10^{-2})	±99%CI
46-48	**-.670**	-1.805 ±	.785	.966	3.865 ±	.405	-.602	-8.937 ±	4.659	.315	1.016 ±	1.215
44-46	**-.834**	-2.625	.681	.958	.968	.144	-.646	-2.073	.963	**.922**	1.172	.196
42-44	.469	.500	.370	.969	1.427	.142	**.484**	6.682	4.748	-.570	-1.781	1.020
40-42	.897	3.061	.592	-.380	-.256	.247	-.037	-.073	.783	.371	6.596	6.564
38-40	**-.923**	-2.271	.372	**-.791**	-.489	.149	**.631**	1.587	.266	**.472**	2.252	.167
36-38	**-.992**	-5.556	.284	**-.975**	-1.126	.100	**.958**	1.976	.231	-.720	-2.661	1.019
34-36	**-.986**	-5.130	.343	**-.852**	-.894	.216	**.814**	1.642	.461	-.294	-5.270	6.800
Bight	**-.850**	-3.686	.897	**-.436**	-.414	.335	**.819**	1.790	.493	.092	.671	2.902
30-32	-.378	-1.053	1.014	**-.433**	-1.100	.900	**.945**	8.605	1.175	-.147	-1.040	2.786
28-30	-.338	-1.296	1.416	-.275	-.264	.140	**.950**	2.374	.306	.334	.446	.501
26-28	.710	1.399	.545	.507	.461	.308	**.789**	3.644	1.113	.257	.935	1.399
24-26	.955	3.263	.406	.801	.794	.233	**.780**	2.261	.712	**.602**	1.200	.635
22-24	.809	1.627	.465	.992	2.658	.130	**.803**	10.700	3.116	**.816**	4.129	1.161

Table 2: Correlations (r) and slopes (b) of linear fits (y = a + bx) of averaged April-July upwelling series values for northward wind stress (t) (m^2/s^2) against year, SST (°C) against year, and SST against northward wind stress, and SST against northward stress for October-January series, for period 1946-90 for 2° COADS data. Dependent (y) variable listed first. The 99% confidence intervals are given. The .01 (.05) significance level on r is .397 (.302), n=45 for Apr-Jul series; .402 (.306), n=44 for Oct-Jan series. Bold values of r denote linear regression is significant at .01 level, and of the sign consistent with increased upwelling (decreasing τ, SST over time; decreasing SST vs. τ). Bold latitudes denote regions where all three linear regressions are significant and of the sign consistent with increased upwelling.

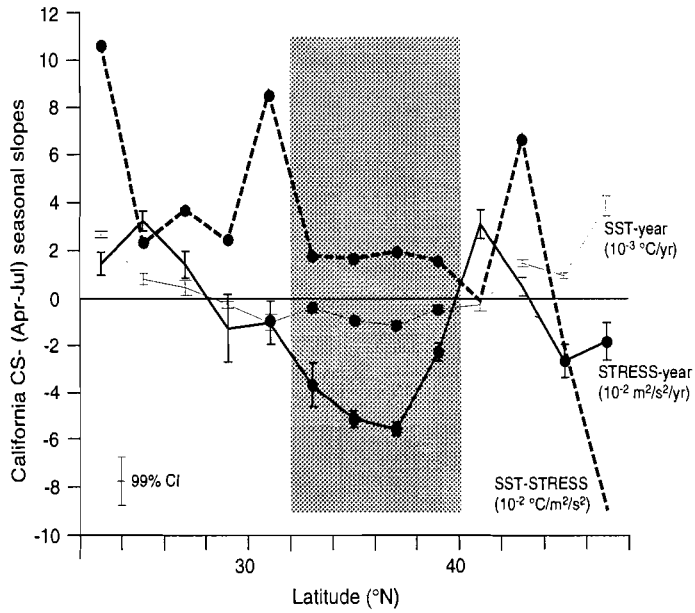

Fig. 3: Slopes (*b*) of linear fits (y = a + *bx*) of averaged April-July upwelling series values for northward wind stress (τ) (m^2/s^2) against year (bold solid line), SST (°C) against year (light solid line), and SST against northward wind stress (dashed line), for period 1946-90 for 2° COADS data. The 99% confidence intervals are shown. Solid circles denote linear regression is significant at .05 level. Shading denotes region where all three linear regressions for a COADS box are significant and of the sign consistent with increased upwelling. Horizontal axis is 10^{-3} $m^2/s^2/yr$ for stress vs. time, 10^{-3} ° for SST vs. time, and 10^{-2} °C/ m^2/s^2 for SST vs. stress.

2.2. A comparison of shore-based seasonal series to the COADS series

All coastal upwelling (April-July seasonal) SST and sea level series decreased over time and all SSS series increased over time, implying an increase in upwelling (Fig. 4, Table 4). The magnitude of their changes corresponds to about 0.07-0.14°C, 0.01-0.1 ppt, and 0.1-0.7cm over the past 45 years. Correlations versus time are all highly significant ($p < .01$). Except for Crescent City, where the adjacent COADS stress (41N) shows an increasing seasonal trend, SST and sea level (SSS) are highly positively (negatively) correlated with local wind stress (Table 3). The patterns occurring during the period covered by the COADS data (1946-90) are consistent with those seen in the full-length shore series (57-78 years) (Table 5). Regressions between coastal SST, SSS and sea level (the series shown in Fig. 4) are highly significant and of the sign consistent with that expected if upwelling is the controlling process (Tables 3, 6). This is consistent with the fact that upwelling is a dominant process off much of the west coast during April-July.

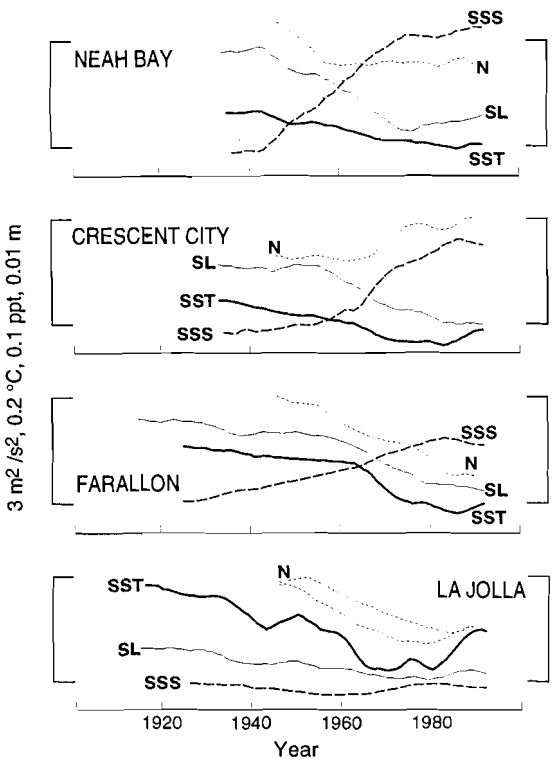

Fig. 4: Time series plots of 'upwelling' series (April-July averages from seasonal model components) for shore SST (bold solid lines), sea level (SL, light solid lines), surface salinity (SSS, bold dashed lines), and COADS poleward wind stress (τ), light dotted lines), for Neah Bay, WA (vs. 46-48°N τ), Crescent City, CA (vs. 40-42°N τ), Farallon, CA (vs. 36-38°N τ), and La Jolla, CA (vs. Southern California Bight τ). Vertical axes denote 0.2°, 0.1 ppt, 0.01m, and 3 m^2/s^2, respectively. Refer to Fig. 1 for location of shore stations.

STATION	SST vs. τ		SSS vs. τ		SL vs. τ	
	r	b (10^{-2})	r	b (10^{-3})	r	b (10^{-3})
NEAH BAY	**.656**	3.415±1.542	**-.764**	-72.178±23.951	**.715**	4.601±1.766
CRESCENT	-.827	-4.047±1.082	.936	64.961±9.596	-.890	-4.200±.844
FARALLON	**.944**	11.28±2.729	**-.966**	-1.920±.202	**.971**	2.638±.256
LA JOLLA	**.892**	5.777±1.150	**-.645**	-4.264±1.983	**.966**	.918±.097

Table 3: Correlations (r) and slopes (b) of linear fits of averaged April-July upwelling series values for coastal SST (°C), salinity (SSS) (ppt), and sea level (SL) (m) against northward wind stress (τ) (m^2/s^2) in adjacent 2° COADS regions, for period 1946-90. Dependent (y) variable listed first. Results shown for Neah Bay, WA (vs. 46-48°N τ), Crescent City, CA (vs. 40-42°N τ), Farallon, CA (vs. 36-38°N τ), and La Jolla, CA (vs. So. Cal. Bight τ). The 99% confidence intervals are given. The .05 (.01) significance level on r is .302 (.397), n=45. Bold values of r denote linear regression is significant at .05 level, and of the sign consistent with increased upwelling (increasing SST and SL, decreasing SSS, vs. τ). Bold stations denote locations where all three linear regressions are significant and of the sign consistent with increased upwelling.

STATION	SST vs. YEAR		SSS vs. YEAR		SL vs. YEAR	
	r	b (10^{-3})	r	b (10^{-4})	r	b (10^{-4})
NEAH BAY	**-.972**	-1.362±.129	**.959**	24.416±2.820	**-.919**	-1.591±.269
CRESCENT	**-.898**	-1.500±.289	**.981**	23.235±1.794	**-.974**	-1.568±.143
FARALLON	**-.958**	-3.009±.355	**.976**	10.870±.955	**-.981**	-1.493±.116
LA JOLLA	**-.566**	-1.589±.910	**.775**	2.219±.712	**-.728**	-.300±.111

Table 4: Correlations (r) and slopes (b) of linear fits of averaged April-July upwelling series values for Neah Bay, Crescent City, Farallon, and La Jolla SST (°C), SSS (ppt), and sea level (m) against year, or period 1946-90 for 2° COADS data. Dependent (y) variable listed first. The 99% confidence intervals are given. The .05 (.01) significance level on r is .302 (.397), n=45. Bold values of r denote linear regression is significant at .05 level, and of the sign consistent with increased upwelling (decreasing SST and SL, increasing SSS over time). All three linear regressions are significant and of the sign consistent with increased upwelling at all four locations.

An examination of the April-July seasonal averages at other coastal stations reveals very similar patterns (Fig. 5). Note the high degree of visual correlation between coastal SST series in adjacent boxes and along the entire coast. Several stations along the central and southern California coast (e.g., Avila, Bodega), over the 32-40°N range of increased upwelling suggested by the COADS data, feature decreasing SST and increasing SSS. These time series agree quantitatively with the other coastal sites discussed previously, both in the linear tendency and the decadal period fluctuations. Upwelling SST and SSS series generated for coastal stations north of 50°N (e.g., Cape St. James, British Columbia; Seward, Alaska) display no statistical change during April-July, suggesting the patterns of increased upwelling noted in the center of the CCS are not evident in the subarctic Pacific region influenced by the Alaskan Gyre.

The correlations between COADS and coastal SST are significant, although the slopes of the linear regressions between shore-based SST and COADS stress series are larger than with the COADS SST (Tables 3, 6); i.e., shore SST changes are

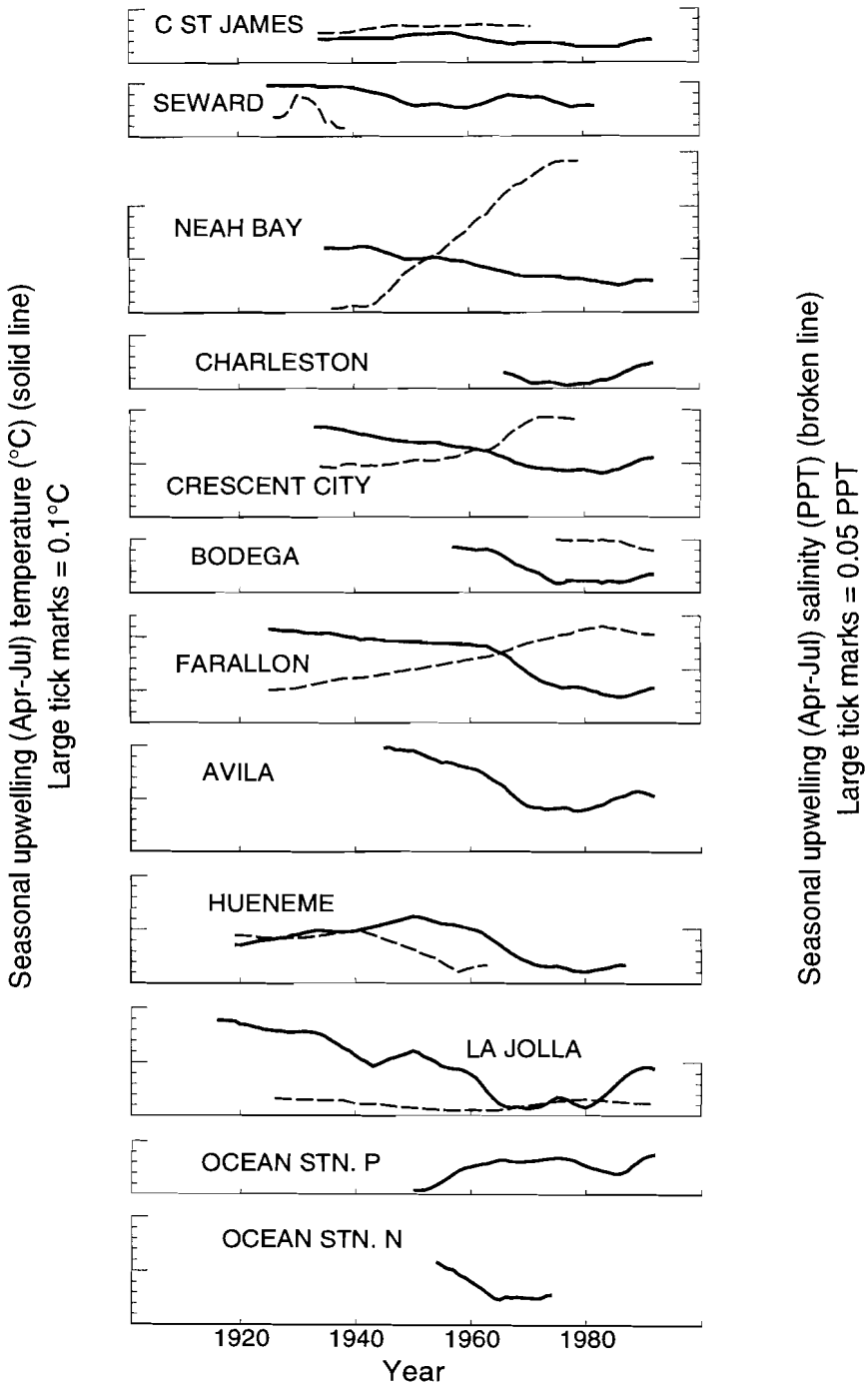

Fig. 5: Time series plots of 'upwelling' series (April-July averages from seasonal model components) for shore SST (solid lines) and SSS (dashed lines), for representative shore stations along the North American coast, and Ocean Stations N and P. Large tick marks on vertical axes denote 0.1°C and 0.05 ppt, respectively. Refer to Fig. 1 and Table 1 for location of shore stations.

greater than COADS SST changes. One exception is the negative correlation between the COADS and coastal SST at Neah Bay. The differences between the linear slopes of SST at the coast and COADS SST, which integrates SST over a large offshore area, probably are due to the dilution of coastal upwelling in the offshore domain of the COADS boxes.

To test whether these tendencies in the seasonal series are a coastal phenomenon, or possibly basin-wide, upwelling series were constructed from the seasonal model components of time series of SST and SSS at Ocean Station P (OSP), and SST at Ocean Station N (OSN) (Fig. 1, Table 1). The upwelling series at OSP (Fig. 5), located in the West Wind Drift, an eastward current that separates into the California Current and the Aleutian Current, reflect an increasing SST and SSS over time (Table 5), implying an increase in the contribution of subtropical water. This pattern does not reconcile with that seen in the CCS downstream of this ocean site, thus it is not likely linked with the COADS results.

SST at OSN, located in the subtropical North Pacific well to the west of the CCS, displays a clear cooling tendency of the same magnitude as the coastal sites, and looks quite similar to coastal SST series over its relatively short (21 years) record length (Fig. 5). Its position rules out changes in coastal upwelling as an explanation for this pattern. However changes in the wind curl over the eastern Pacific, which could lead to an intensification in Ekman pumping at locations remote from the coast, are a possibility. The hypothesized intensification of the thermal continental low in summer, which would contribute to increased coastal upwelling, could lead to changes in the wind gradients in the region of OSN as well. While an investigation of this possibility is beyond the scope of this paper, it is nevertheless an intriguing question, given the similarity between the coastal and OSN SST upwelling series. Closer analysis may suggest mechanisms by which long-term basin-scale forcing variability may impact upper ocean circulation patterns, and possibly coastal upwelling processes.

While the majority of the upwelling series display a highly linear tendency over time, some series exhibit considerable variability on decadal scales that is consistent within adjacent areas. For example, shore SSTs shift suddenly to more rapid cooling in early 1960s, to a slower rate of decreasing SST a few years later, and appears to reverse around 1980 (Fig. 5); SSS shows the opposite pattern. Non-linear upwelling series should not be construed as lacking a climate signal. Climate variability is not monotonic (e.g., the dramatic 1976 climate shift over the north Pacific (Trenberth, 1990; Graham, 1994; Trenberth and Hurrell, 1994)). Many of the series have variability such that truncating their length by even a few years leads to substantially different linear tendencies. A key result here is their consistency within geographical regions, such as the 32-40°N area dominated by coastal upwelling.

STATION	SST vs. YEAR		SSS vs. YEAR		SL vs. YEAR	
	r	b (10^{-3})	r	b (10^{-4})	r	b (10^{-4})
NB	**-.976**	-1.378±.105(58)	**.993**	38.379±1.798(44)	**-.943**	-1.569±.189(59)
CC	**-.926**	-1.473±.204(60)	**.928**	11.942±1.867(46)	**-.949**	-1.205±.135(60)
FAR	**-.942**	-2.124±.240(68)	**.985**	9.760±.540(68)	**-.949**	-.953±.093(78)
LJ	**-.853**	-2.028±.369(77)	-.068	-.131±.615(67)	**-.920**	-.403±.051(78)
OSP	.581	.859±.484(43)	**.844**	1.173±.325(37)	—	—
OSN	**-.881**	-3.285±1.043(21)	—	—	—	—

Table 5: As above, for entire series (n shown in parentheses next to 95% CI).

3. DISCUSSION

Strong evidence of a systematic intensification of upwelling during April--July is seen along the west coast of North America between 32-40°N (Fig. 3, Table 2). This region corresponds with an area where coastal upwelling predominates during spring and summer (Parrish *et al.*, 1981). It is offset slightly south of the primary upwelling region (Point Conception CA-Cape Blanco OR), suggesting that southward advection may account for the distribution of some of the cooling tendencies in COADS SSTs. This is consistent with the small negative SST-stress slope at 41°N, at the northern edge of the upwelling region, as well as the relatively large positive slope at 31°N, the southern boundary of upwelling (Fig. 3). Another large positive slope is seen at 23°N, south of an upwelling center off Baja California (Bakun and Nelson, 1977).

SST during the upwelling season has increased north and south of this region of intensified upwelling. However a corresponding decrease in equatorward stress, implying decreased coastal upwelling, only occurs south of 28°N. Stress is negatively correlated with SST north of 40°N, suggesting that seasonal changes in wind stress are not reflected in SST through coastal upwelling. This is not surprising since this region is at the northern extent of predominantly meridional wind associated with the pressure gradient between the continental low over the western U.S. and the North Pacific High, and is more influenced by predominantly zonal wind stress in the gradient between the High and the Aleutian Low (Bakun and Nelson, 1991). Offshore-directed Ekman surface transport during spring and summer is greatly reduced north of 40°N as well (Parrish *et al.*, 1983), further demonstrating the reduced role of coastal upwelling at northern latitudes.

Regions north of 40°N and south of 32°N are away from the influence of the continental low as well. Bakun (1992) points out that the Gulf of California occupies the area corresponding to the continental interior at higher latitudes. Therefore these areas are less susceptible to any increase in upwelling that would be associated with the intensification of the summer continental low and the subsequent strengthening of equatorward wind stress. Finally, anticyclonic curl dominates in the northern and southern regions, in contrast to strong cyclonic curl off California (Bakun and Nelson, 1991). Anticyclonic curl leads to Ekman convergence and downwelling, countering the effect of offshore Ekman transport and possibly explaining the limited geographical extent of the increased coastal upwelling over the past several decades.

The coastal stations corroborate these results. Four shore stations –Neah Bay, Crescent City, Farallon and La Jolla– have long series of SST, SSS and SL for comparison to the COADS wind (Fig. 4). Farallon is located in the center of the upwelling region on an island about 45 km west of San Francisco (SL for this location was measured at San Francisco). This site is frequently bathed by recently upwelled water from the north (Schwing *et al.*, 1991). An increasing equatorward wind stress corresponds with decreasing SST and SL, and increasing SSS at this location, all consistent with a systematic intensification of upwelling over the past several decades.

The tendencies at Neah Bay are similar to those at Farallon. The same is true at La Jolla; however the rate of change in the series over time is reduced. Coastal upwelling may be increasing in the Bight, but it is either a relatively small change or may be partially masked by other factors that impact the seasonality of the dynamics controlling the Bight's oceanic conditions. At Crescent City, the oceanic variables change in a manner consistent with increased upwelling, despite the fact that wind stress at this latitude has become increasingly poleward. The COADS winds may not be truly representative of the nearshore winds that drive coastal upwelling. Another possibility is that ocean conditions off northern California are controlled by non-local forcing which advects upwelled water south from the Cape Blanco upwelling region. Crescent City is near the divergence point of both the mean wind stress and the tendency of the COADS upwelling series. Ongoing

analysis of wind and SST trends suggests further that the area's wind and SST fields are extremely heterogeneous on space scales of *O(100 km)* at time scales of years-decades (R. Parrish, pers. comm.), which suggest a combination of non-local forcing and complex circulation may be responsible for the seasonal tendencies seen at Crescent City.

Are the seasonal tendencies in wind stress and SST truly limited to the upwelling season, or are they representative of a pattern that occurs throughout the year? The former should be the case, since non-seasonal tendencies will be incorporated into the trend model component. Time series were constructed from the October-January means of the seasonal model series. The slopes of the linear fits of COADS SST to wind stress for these winter seasonal series (Table 2) show a very different pattern from the upwelling season. Only a few isolated COADS boxes reflect a significant positive correlation between SST and stress. Of these, a positive correlation was found for only one box within the 32-40°N upwelling area (39°N), and this was associated with an increasing (reduced upwelling) SST and stress tendencies. From this it can be concluded that the patterns consistent with increasing upwelling limited to the spring and summer. Other physical processes are controlling the seasonal wind and SST tendencies at other times of the year.

Are the regression statistics described above unique to the seasonal model components? The analysis was repeated by examining time series constructed from the April-July averages of the model trends and the monthly observations (raw data). The series constructed from the observations are analogous to those analyzed by Bakun (1990). The wind stress trend series display an increasing equatorward tendency south of 42°N and poleward north of 42°N, a pattern matched by the April-July observations (Fig. 6). The tendencies of the observed and trend series are negative, consistent with the seasonal upwelling series in the region 32-40°N (but at a lower level of significance). However the linear slopes of the trends and observations (*0.1-0.6* $m^2/s^2/yr$) are generally an order of magnitude greater than in the seasonal tendencies (*0.01-0.05* $m^2/s^2/yr$), reflecting the strong bias of the April-July observations toward the long-term trend. Linear tendencies of the CCS geostrophic wind series constructed by Bakun (1990) for April-September are very similar to the trend and observation tendencies reported here, reflecting the fact that long-term trends were incorporated in the «seasonal» series in his analysis.

The April-July trend and observed series south of 36°N display a general warming pattern (Fig. 7), whereas the seasonal upwelling series show a cooling tendency over the region 28-42°N. The wind and SST trend series are significantly correlated only at 39N, which is also the only location where the SST trends have a statistically significant cooling tendency. As with stress, the linear tendencies of the SST trends are *O(10)* and greater than the seasonal tendencies, and generally of opposite sign. Again the observation and trend series correspond closely. The linear regressions off much of California and Baja California imply the seasonal SST component has been cooling at a rate of $-0.5\text{-}1.0 \times 10^{-3}$°C/yr, while the trends in this area exhibit a warming tendency of greater than 10×10^{-3}°C/yr. Schwing (1994) found consistent results from a similar comparison of the Farallon SST and SSS observed, trend and seasonal series. The long-term warming trend masks seasonal cooling associated with increased upwelling during spring and summer off central and southern California. These comparisons reflect the importance of using a method that separates seasonal and long-term contributions to environmental time series, and argue against looking for changing seasonal patterns in direct extractions from observations without properly accounting for the non-linear climate trend. Otherwise long-term climate patterns may be improperly linked to, and even misidentified as, changes in the seasonal cycle.

Because the dynamical relationship between wind forcing and coastal upwelling is the same at any time scale that is long relative to the inertial period, we expect that the SST model trend series should correspond to stress trends in a manner consistent with Bakun's (1990) hypothesis of increased upwelling (e.g., SST displays a cooling trend at locations where the trend suggests increased equatorward stress). A comparison of linear fits to the stress and SST trends (Fig. 6 and 7) shows the correlation between these trends is positive from about 34-42°N, as Bakun (1990) hypothesizes, but negative off the

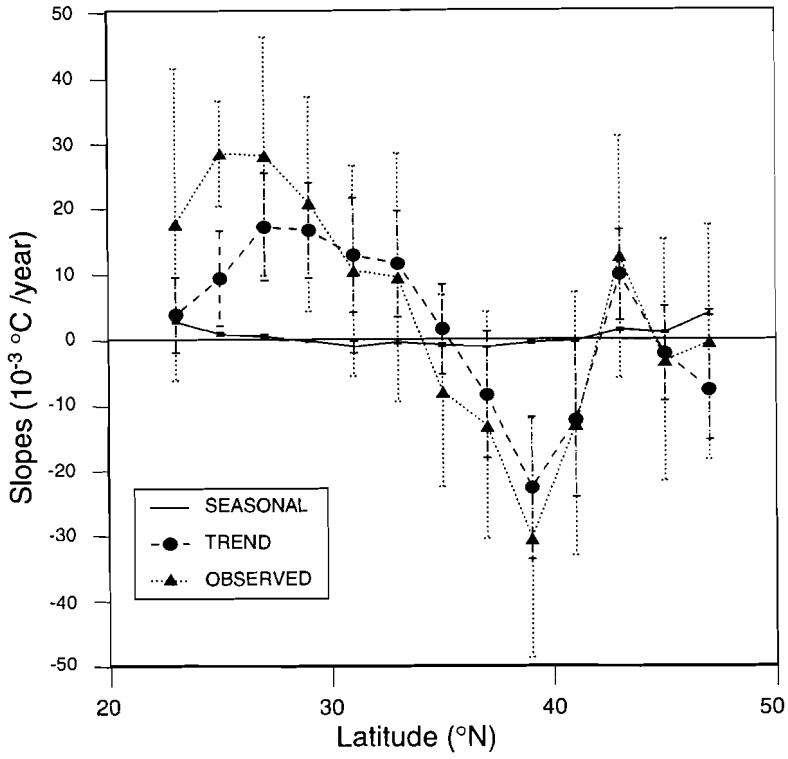

Fig. 6: Slopes (b) of linear fits ($y = a + bx$) of averaged April-July values of 2° COADS data poleward wind stress (m^2/s^2) against year, from monthly observations (dotted line), trend model component (dashed line), and seasonal model component (solid line), for the period 1946-90. The 99% confidence intervals are shown.

northwest U.S., and southern and Baja California. An analysis of the model trends is the focus of another publication (Schwing *et al.*, 1991). It is important however to recognize the difference between changes in the model trend series, which are due to superannual changes over time, and changes in the seasonal series, which are associated with climate variations that favorably affect a certain season or portion of the year. Because wind-driven coastal upwelling is one of several processes that impact SST and other ocean conditions, other factors (e.g., global warming) that may affect upper ocean variability cannot be ignored. The importance of these effects relative to wind forcing differs as a function of time scale. This may account for the different relationship between stress and SST in the trend and seasonal model components. Specifically we conclude that coastal upwelling controls SST in much of the CCS on seasonal scales. Therefore a close relationship exists between the spring/summer seasonal stress and SST series. SST trends, on the other hand, appear less closely linked to changes in local wind stress because factors other than wind forcing contribute significantly to SST variability.

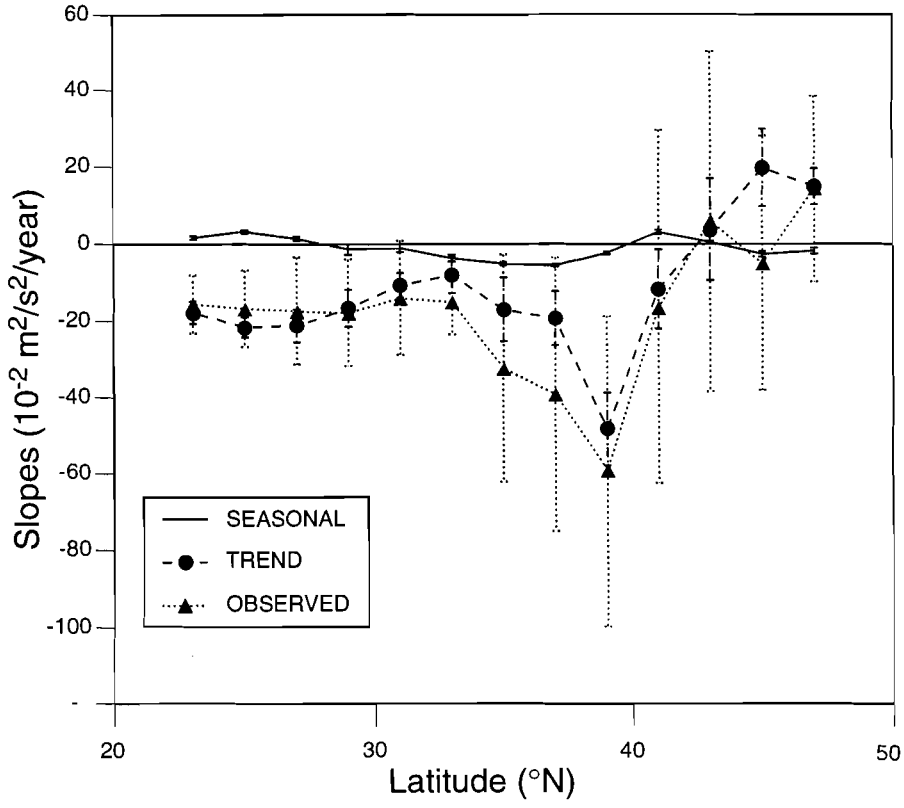

Fig. 7: Slopes (*b*) of linear fits ($y = a + bx$) of averaged April-July values of 2° COADS SST °C) against year, from monthly observations (dotted line), trend model component (dashed line), and seasonal model component (solid line), for period 1946-90. The 99% confidence intervals are shown.

	CSST vs. SST		SSS vs. SST		SST vs. SL		SSS vs. SL	
	r	b	r	b	r	b	r	b
NEAH	-.963	-2.745±.304	**-.977**	-1.774±.153	**.962**	7.778±.871	**-.985**	-14.464±1.007
CRES	**.497**	.203±.139	**-.933**	-1.323±.200	**.945**	9.809±1.330	**-.988**	-14.540±.881
FAR	**.972**	.357±.034	**-.978**	-.347±.029	**.989**	20.410±1.219	**-.988**	-7.226±.453
LA JOLLA	**.950**	.320±.041	**-.442**	-.045±.036	**.943**	64.292 8.862	**-.602**	-4.190±2.179

Table 6: Correlations (r) and slopes (b) of linear fits of averaged April-July upwelling series values for COADS SST (CSST), coastal SST (°C), SSS (ppt), and sea level (m), for period 1946-90. Dependent (y) variable listed first. Results shown for Neah Bay, WA (vs. 46-48°N CSST), Crescent City, CA (vs. 40-42°N CSST), Farallon, CA (vs. 36-38°N CSST), and La Jolla, CA (vs. So. Cal. Bight CSST). The 99% confidence intervals are given. The .05 (.01) significance level on r is .302 (.397), n=45. Bold values of r denote linear regression is significant at .05 level, and of the sign consistent with increased upwelling (decreasing CSST, SST and sea level, increasing SSS).

LATITUDE (°N)	SEASONAL τ vs. YEAR		TREND τ vs. YEAR		OBSERVED τ vs. YEAR	
	r	b (10^{-2}) ±99%CI	r	b (10^{-2}) ±99%CI	r	b (10^{-2}) ±99%CI
46-48	**-.670**	-1.805±.785	.781	14.892±4.682	.228	14.362±24.148
44-46	**-.834**	-2.625±.681	.614	19.718±9.961	-.060	-5.050±33.003
42-44	.469	.500±.370	.112	3.760±13.142	.053	5.974±44.337
40-42	.897	3.061±.592	**-.409**	-11.703±10.268	-.140	-16.557±46.009
38-40	**-.923**	-2.271±.372	**-.893**	-48.468±9.605	**-.499**	-59.258± 40.476
36-38	**-.992**	-5.556±.284	**-.730**	-19.280±7.103	-.396	-39.169±35.689
34-36	**-.986**	-5.130±.343	**-.627**	-17.002±8.288	-.394	-32.457±29.702
Bight	**-.850**	-3.686±.897	**-.562**	-8.026±4.641	**-.570**	-15.043±8.523
30-32	-.378	-1.053±1.014	**-.792**	-10.649±3.227	-.347	-14.007±14.871
28-30	-.338	-1.296±1.416	**-.803**	-16.611±4.850	**-.450**	-17.839±13.892
26-28	.710	1.399±.545	**-.888**	-21.280±4.340	**-.438**	-17.428±14.051
24-26	.953	3.263±.406	**-.956**	-21.663±2.615	**-.551**	-16.765±9.982
22-24	.809	1.627±.465	**-.922**	-17.776±2.940	**-.629**	-15.598±7.577

Table 7: Correlations (r) and slopes (b) of linear fits (y = a + bx) of averaged April-July upwelling series values for northward wind stress (τ) (m^2/s^2) against year, from seasonal and trend model series, and from monthly observed time series, for period 1946-90 for 2° COADS data. Dependent (y) variable listed first. The 99% confidence intervals are given. The .01 (.05) significance level on r is .397 (.302), n=45. Bold values of r denote linear regression is significant at .01 level, and of the sign consistent with increased upwelling (decreasing τ over time).

CONCLUSION

State-space models are applied to multi-decadal monthly-averaged time series of poleward wind stress, sea surface temperature, coastal salinity, and coastal sea level from the California Current System. The period of analysis is 1946-90. The models estimate a non-stationary non-deterministic seasonal component, a non-parametric non-linear trend, and an AR(1) series for each time series of monthly observations using a combination of Kalman filtering and maximum likelihood methods. Our objective here is to examine the variability of the seasonal patterns of coastal upwelling during spring and summer in the CCS, over climate (long-term) time scales. Specifically we test the hypothesis of Bakun (1990) that a long-term global warming trend has led to increasing equatorward wind stress along the west coast of North America, which has resulted in increased rates of coastal upwelling.

The results show a clear separation of the seasonal signal from the trend for wind stress, SST, salinity and sea level. The utility of estimating non-stationary seasonal patterns –using the state-space models– is demonstrated with the finding of a systematic increase in equatorward wind stress, decrease in SST and sea level, and increase in salinity during spring and summer, evidence that coastal upwelling has been increasing in intensity. Significant regional differences in the seasonal series were found. Evidence of increased upwelling is strongest and most prevalent in areas where seasonal coastal

upwelling is a dominant process (e.g., 32-40°N). Shifts in the phase and amplitude of the seasonal cycle over several decades are suggested with this technique as well. This pattern of increasing upwelling intensity over time cannot be discerned in the monthly observations or trend model series. Evidence of increased upwelling is not found in fall-winter, either.

The state-space model appears to be a powerful tool for separating the interannual-to-interdecadal fluctuations in environmental time series from seasonal patterns of variability. The model results help provide a better understanding of the linkages between long-term variations in atmospheric forcing and the coastal ocean's response to this variability, as well as the potential contribution of natural and anthropogenic signals, and regional differences in these effects. The results presented here demonstrate the importance of evaluating temporal and spatial variability over the entire spectrum, rather than simply at global climate scales, when examining long-term environmental fluctuations. They also demonstrate the importance of considering independently the change in seasonal patterns versus changes in the long-term climate trend.

REFERENCES CITED

Bakun A. 1990. Global climate change and intensification of coastal ocean upwelling. *Science*, 247: 198-201.

Bakun A. 1992. Global greenhouse effects, multi-decadal wind trends, and potential impacts on coastal pelagic fish populations. *ICES Mar. Sci. Symp.*, 195: 316-325.

Bakun A. and C.S. Nelson. 1977. Climatology of upwelling related processes off Baja California. *CalCOFI Reports*, 19: 107-127.

Bakun A. and C.S. Nelson. 1991. The seasonal cycle of wind-stress curl in subtropical eastern boundary current regions. *J. Phys. Oceanogr.*, 21: 1815-1834.

Cardone V.J., J.G. Greenwood and M. Cane. 1990. On trends in the historical marine wind data. *J. Climate*, 3: 113-127.

Cayan D.R., D.R. McLain, W.D. Nichols, and J.S. DiLeo-Stevens. 1988. *Monthly climatic time series data from the Pacific Ocean and western Americas.* USGS Open-File Report, 379p.

Cury P. and C. Roy. 1989. Optimal environmental window and pelagic fish recruitment success in upwelling areas. *Can. J. Fish. Aquat. Sci.*, 46: 670-680.

Graham N.E. 1994. Decadal scale variability in the 1970's and 1980's: observations and model results. *Clim. Dyn.*, 10: 60-70.

Harvey A.C. 1989. Forecasting, structural time series models and the Kalman filter. Cambridge University Press, Cambridge, 554p.

Isemer H.-J. 1992. Comparison of estimated and measured marine surface wind speed. *In*: H.F. Diaz, K. Wolter and S.D. Woodruff (eds.). *Proceedings of the International COADS Workshop*, Boulder, Colorado, 13-15 January 1992. U.S. Dept. of Commerce. 142-158.

Mann M.E. and J. Park. 1993. Spatial correlations of interdecadal variation in global surface temperatures. *Geophys. Res. Lett.*, 20: 1055-1058.

Mann M.E. and J. Park. 1994. Global-scale modes of surface temperature variability on interannual to century timescales. *J. Geophys. Res.*, 99: 25819-25833.

Mendelssohn R. and C. Roy. 1996. Comprehensive Ocean Data Extraction. Users Guide, U.S. Dep. comm., NOAA Tech. Memo. NOAA Tech. Rep. NMFS SWFSC, La Jolla, CA., 228, 67p.

Miller A.J., D.R. Cayan, T.P. Barnett, N.E. Graham and J.M. Oberhuber. 1994. Interdecadal variability of the Pacific Ocean: model response to observed heat flux and wind stress anomalies, *Clim. Dyn.*, 9: 287-302.

Parrish R.H., C.S. Nelson and A. Bakun. 1981. Transport mechanisms and reproductive success of fishes in the California Current. *Biol. Oceanogr.*, 1: 175-203.

Parrish R.H., A. Bakun, D.M. Husby and C.S. Nelson. 1983. Comparative climatology of selected environmental processes in relation to eastern boundary current fish production. *FAO Fish Rep.*, 291: 731-778.

Roemmich D. 1992. Ocean warming and sea level rise along the southwest U.S. coast. *Science*, 257: 373-375.

Rosenfeld L.K., F.B. Schwing, N. Garfield and D.E. Tracy. 1994. Bifurcated flow from an upwelling center: a cold water source for Monterey Bay. *Continental Shelf Research*, 14: 931-964.

Schwing F.B. 1994. Long-term and seasonal patterns in coastal temperature and salinity along the North American west coast. *In*: K.T. Redmond and V.L. Tharp (eds.). *Proceedings of the Tenth Annual Pacific Climate (PACLIM) Workshop*. Interagency Ecological Studies Program for the Sacramento-San Joaquin Estuary. Tech. Rep., 36: 129-143.

Schwing F.B., D.M. Husby, N. Garfield and D.E. Tracy. 1991. Mesoscale oceanic response to wind events off central California in spring 1989: CTD surveys and AVHRR imagery. *CalCOFI Reports*, 32: 47-62.

Shumway R.H. 1988. *Applied statistical time series analysis*. Prentice-Hall, Englewood Cliffs, 379p.

Slutz R.J., S.J. Lubker, J.D. Hiscox, S.D. Woodruff, R.L. Jenne, D.H. Joseph, P.M. Steurer and J.D. Elms. 1985. *Comprehensive Ocean-Atmosphere Data Set*. Release 1. NOAA Environmental Research Laboratories, Climate Research Program, Boulder, CO. 268p.

Trenberth K.E. 1990. Recent observed interdecadal climate changes in the northern hemisphere. *Bull. Am. Meteor. Soc.*, 71: 988-993.

Trenberth K.E. and J.W. Hurrell. 1994. Decadal atmospheric-ocean variations in the Pacific. *Clim. Dyn.*, 9: 303-319.

Walker P.M., D.M. Newton and A.W. Mantyla. 1993. *Surface water temperatures, salinities and densities at shore stations, United States West Coast, 1992*. University of California, San Diego, Scripps Institution of Oceanography, La Jolla, CA, SIO Ref. 93-18, 46p.

Ware D.M. 1995. A century and a half change in the climate of the NE Pacific. *Fish. Oceanogr.*, 4: 267-277.

Woodruff S.D., R.J. Slutz, R.L. Jenne and P.M. Steurer. 1987. A Comprehensive Ocean-Atmosphere Data Set. *Bull. Am. Meteor. Soc.*, 68: 1239-1250.

Wu Z. and R.E. Newell. 1992. The wind problem in COADS and its influence on the water balance. *In*: H.F. Diaz, K. Wolter and S.D. Woodruff (eds.). *Proceedings of the International COADS Workshop*, Boulder, Colorado, 13-15 January 1992. U.S. Dept. of Commerce: 189-200.